

# Moments of parton distribution functions of any order from lattice QCD

Andrea Shindler\*

*Institute for Theoretical Particle Physics and Cosmology, TTK, RWTH Aachen University  
Nuclear Science Division, Lawrence Berkeley National Laboratory, Berkeley, CA 94720, USA and  
Department of Physics, University of California, Berkeley, CA 94720, USA*

(Dated: December 1, 2023)

We describe a procedure to determine moments of parton distribution functions of any order in lattice QCD. The procedure is based on the gradient flow for fermion and gauge fields. The flowed matrix elements of twist-2 operators renormalize multiplicatively, and the matching with the physical matrix elements can be obtained using continuum symmetries and the irreducible representations of Euclidean 4-dimensional rotations. We calculate the matching coefficients at one-loop in perturbation theory for moments of any order in the flavor non-singlet case. We also give specific examples of operators that could be used in lattice QCD computations. It turns out that it is possible to choose operators with identical Lorentz indices and still have a multiplicative matching. One can thus use twist-2 operators exclusively with temporal indices, thus substantially improving the signal-to-noise ratio in the computation of the hadronic matrix elements.

**Introduction** - Quantum Chromodynamics (QCD), the theory of strong interactions, comprehensively describes the interactions between quarks and gluons across a broad energy spectrum, including the binding mechanisms between these elementary particles. QCD is non-perturbative at low energies, presenting a challenge in applying perturbative methods for the analysis of hadron structures.

The study of hadron structure relies on the parton picture, where the dynamics of quarks and gluons are characterized by parton distribution functions (PDF). The precision of QCD calculations is intricately tied to the accuracy of these PDFs, and this connection plays a crucial role in current measurements at the LHC. It will continue to be essential for future investigations at the EIC, HL-LHC, and LHeC. The current and future search for new physics depends heavily on the precision of the comparison between experimental data and theoretical predictions. This underscores the importance of a precise determination of PDFs.

The understanding of collider processes based on QCD factorization allows for the study of hadron structure using PDFs. Going beyond PDFs, generalized parton distributions (GPDs), and transverse-momentum-dependent distributions (TMDs) complement the 3-D description of hadrons. Although all the distribution functions are not directly measurable, they can be determined by factorizing the hard and soft parts of the cross-section of the process of interest.

In deep inelastic scattering (DIS), a key role is played by the structure functions,  $F_k(x, Q^2)$  ( $k = 1, 2, 3$ ), which depend on  $Q^2 = -q^2$ , where  $q$  is the 4-momentum transferred to the nucleon, and  $x = Q^2/2(pq)$  represents the fraction of nucleon momentum carried by the parton. Here,  $p$  denotes the nucleon momentum. For  $Q^2$  much

larger than the nucleon mass, the factorization theorem [1]

$$F_k(x, Q^2) = \sum_a C_k^a(Q^2/\mu^2) \otimes f_a(x, \mu^2), \quad (1)$$

relates the structure functions to the convolution of the scale-dependent parton distribution functions  $f_a(x, \mu^2)$  with the Wilson coefficients  $C_k^a(Q^2/\mu^2)$  (summed over quark flavors and gluons,  $a$ ). The Wilson coefficients are calculable in perturbation theory, and the evolution of the PDFs in  $\mu$  is governed by the Dokshitzer-Gribov-Lipatov-Altarelli-Parisi (DGLAP) equations [2–5]. The DGLAP equations can be solved once we specify an initial condition at a certain scale  $\mu = \mu_0$ . The evolution of the PDFs is calculable in perturbation theory, but the precision of experimental data always necessitates higher-order calculations. The standard choice for renormalization and factorization scheme is the  $\overline{\text{MS}}$  scheme. PDFs can be determined experimentally by analyzing a set of hard-scattering processes involving nucleons. There is a long-standing community effort to determine PDFs using well-defined parametrizations for their  $x$ -dependence and starting the evolution around  $\mu_0^2 = 1 - 4\text{GeV}$ .

Lattice QCD can offer a theoretical input for the determination of the PDFs and their evolution. The direct calculation of PDFs using lattice QCD poses particular challenges due to the Euclidean geometry and the light-cone dominance of the kinematics. The connection between PDFs and hadronic matrix elements, which are calculable in lattice QCD, is established through the moments of the PDFs, denoted as  $\langle x^n \rangle$  [6, 7]. Lattice QCD calculations of the moments of the PDFs, pioneered in Refs. [8–10], provide, in principle, a means for the complete reconstruction of the PDFs. This possibility has remained impractical due to the theoretical and numerical challenges associated with computing high moments. Alternative approaches have been developed to determine the  $x$ -dependence of the PDFs, including the heavy-quarks OPE [11, 12], the quasi-PDF [13], the pseudo-PDF [14], the OPE-based method of [15], the current-current approach [16], and the hadron tensor method of [17].

\* shindler@physik.rwth-aachen.de

Different high-energy scatterings are associated with different PDFs: unpolarized, helicity, and transversity. Certain kinematical regions, as well as specific PDFs, pose challenges for extraction from experimental data. This emphasizes the significance of reconstructing the PDFs from lattice QCD simulation data.

In this work, we revisit the possibility of calculating moments of PDFs, which, if successful, would provide an important and complementary approach to determine distribution functions from QCD. We describe a method that addresses both the theoretical and numerical challenges faced in the past, which hindered the calculation of moments of any order from lattice QCD.

**Twist-2 operators** - QCD factorization, as expressed in Eq. (1), relates the moments of the structure functions and the moments of the parton distribution functions. Taking the example of  $F_1$ , the relation is given by e.g.

$$\int_0^1 dx x^{n-1} F_1(x, Q^2) = \sum_a C_{1,n}^a(Q^2, \mu^2) A_n^{a/h}(\mu) \quad (2)$$

where  $A_n^{a/h}(\mu)$  represents the reduced matrix element of certain local operators, denoted by  $O_n$ , between the hadron states, denoted as  $h$ , and  $C_{1,n}^a(Q^2, \mu^2)$  are the corresponding Wilson coefficients, calculable in perturbation theory. In the context of DIS kinematics, the leading contribution, given in Eq. (2), arises from local operators with the lowest twist,  $\tau = d_O - n = 2$ , where  $d_O$  is the physical dimension of the local operator and  $n$  is its spin. In the parton model the reduced matrix element is related to the moments of the PDFs,  $A_n^{a/h} = \langle x^{n-1} \rangle_{a/h}$  [6, 7].

The form of the local operators  $O_n$  can be constrained by requiring that they belong to irreducible representations of the Lorentz group. This guarantees that the renormalization procedure does not generate mixing with operators of the same or lower dimensions. Lattice QCD simulations are performed in a Euclidean setup though, and the symmetry group in a Euclidean lattice is the hyper-cubic group  $H(4)$ . The reduced symmetry does not protect the operators from a complicated mixing pattern, that gets more complicated for larger  $n$ . Once the continuum limit has been performed one recovers  $O(4)$  symmetry.

We now briefly review how to construct irreducible representations of  $O(4)$ . Although this is standard material (see, for example, Ref. [18]), it is useful because it provides the basis to construct the operators that should be used in lattice QCD computations.

A rank- $n$  tensor, denoted as  $T_{\mu_1 \dots \mu_n}$ , belongs to an irreducible representation of the general linear group  $GL(4)$  once the vector indices are symmetrized

$$T_{\{\mu_1 \dots \mu_n\}} = \frac{1}{n!} \sum_{\substack{\sigma \in \text{all} \\ \text{permutations}}} T_{\mu_{\sigma(1)} \dots \mu_{\sigma(n)}}. \quad (3)$$

In the case of the  $O(4)$  group symmetry, tensors with given symmetries do not represent irreducible representations because an additional operation is allowed that

commutes with the orthogonal transformations. If we contract 2 indices, e.g. (12), of the rank- $n$  tensor

$$T_{\mu_1 \dots \mu_n}^{(12)} = T_{\alpha\alpha\mu_3 \dots \mu_n} = \delta_{\mu_1\mu_2} T_{\mu_1 \dots \mu_n}, \quad (4)$$

we obtain a tensor with rank  $n - 2$  and the  $O(4)$  transformation commutes with the operation of contraction. We can repeat the contraction operation for any pair of vector indices, obtaining  $n(n - 1)/2$  traces. The subspace of the rank- $n$  tensors for which all pairs of traces are zero is invariant under  $O(4)$  rotation, and it can be shown that every rank- $n$  tensor can always be decomposed in a tensor with vanishing trace, denoted as  $\hat{T}$ , and a linear combination of  $n(n - 1)/2$  terms of all possible traces

$$T_{\mu_1 \dots \mu_n} = \hat{T}_{\mu_1 \dots \mu_n} + \delta_{\mu_1\mu_2} T_{\mu_1 \dots \mu_n}^{(12)} + \dots \quad (5)$$

This decomposition is invariant under  $O(4)$  transformations. For  $n = 2$  the decomposition is very easy to obtain and the traceless tensor reads

$$\hat{T}_{\mu_1\mu_2} = T_{\mu_1\mu_2} - \frac{1}{4} \delta_{\mu_1\mu_2} T_{\alpha\alpha}. \quad (6)$$

For  $n = 3$ , we have 3 different traces, and the traceless part of the tensor can be computed in the same way

$$\begin{aligned} \hat{T}_{\mu_1\mu_2\mu_3} &= T_{\mu_1\mu_2\mu_3} - \\ &- \frac{1}{6} [\delta_{\mu_1\mu_2} T_{\alpha\alpha\mu_3} + \delta_{\mu_1\mu_3} T_{\alpha\mu_2\alpha} + \delta_{\mu_2\mu_3} T_{\mu_1\alpha\alpha}]. \end{aligned} \quad (7)$$

Traceless tensors are invariant under vector index permutations and can be used as a starting point to construct all the irreducible representations of  $O(4)$  using Young symmetrizers [18]. For the purpose of this work, the only relevant result is that traceless and symmetrized rank- $n$  tensors are an irreducible representation of  $O(4)$ .

We restrict ourselves to unpolarized structure functions, meaning that we consider hadronic matrix elements averaged over the hadron polarization. Other moments of different distributions can be studied using the same procedure described here. We further limit our consideration to flavor non-singlet operators to avoid mixing with gluonic operators, but the same method is applicable to singlet operators.

We consider the following set of operators

$$O_n^{rs}(x) = O_{\mu_1 \dots \mu_n}^{rs}(x) = \bar{\psi}^r(x) \gamma_{\{\mu_1} \overleftrightarrow{D}_{\mu_2} \dots \overleftrightarrow{D}_{\mu_n\}} \psi^s(x). \quad (8)$$

with quark fields,  $\psi^r$ , of different flavors,  $r \neq s$ , and the covariant derivative  $D_\mu = \partial_\mu + G_\mu$ , where  $G_\mu$  represent the gluon field. The symmetrization of the covariant derivative  $\overleftrightarrow{D}_\mu = \frac{1}{2} \left( \overrightarrow{D}_\mu - \overleftarrow{D}_\mu \right)$  guarantees a definite transformation under charge conjugation.

In the continuum, traceless non-singlet twist-2 operators, with symmetrized Lorentz indices, renormalize multiplicatively. For example, in the  $\overline{\text{MS}}$  scheme, the bare operator  $O_{n,B}^{rs}$  renormalizes as follows

$$O_n^{rs}(x) = Z_n^{\overline{\text{MS}}} O_{n,B}^{rs}(x), \quad (9)$$

with renormalization constant  $Z_n^{\text{MS}}$ . The intrinsic non-perturbative nature of the hadronic matrix elements suggests the use of lattice QCD. However, the breaking of the rotational group symmetry into the hypercubic group  $H(4)$  adds complications to the renormalization.

On an hypercubic lattice, the Lorentz indices of the twist-2 operators must be chosen while considering the reduced hypercubic symmetry group  $H(4)$ . Irreducible representations of  $O(4)$  generally become reducible representations of  $H(4)$  inducing unwanted mixings under renormalization [8, 9, 19, 20]. The irreducible representations of  $H(4)$  allow mixings with lower-dimensional operators, and, additionally, complicate the mixing with operators of the same dimensions. A notable example of this complication occurs with the operator  $O_3$ . In the continuum, after symmetrizing over the Lorentz indices and subtracting the traces to obtain  $\widehat{O}_3$ , the renormalization is multiplicative (e.g. in the MS scheme). However, on the lattice, terms like  $1/a^2 \delta_{\mu_i \mu_j} \cos(ap_{\mu_j})$  are allowed by  $H(4)$  symmetry and cannot be removed even after subtracting the trace [8]. This pertains to the fact that  $O_3$  belongs to different irreducible representations of  $H(4)$  depending on the choice of the Lorentz indices. The operator  $O_3$  with all the indices equal, i.e.  $\mu_1 = \mu_2 = \mu_3$ , mixes with the lower-dimensional vector current, causing a power divergence proportional to  $1/a^2$ . For the operators with  $\mu_1 \neq \mu_2 = \mu_3$ , such as the irreducible representation  $O_{411} - O_{433}$ , the renormalization is multiplicative.<sup>1</sup> We note that while  $O_{411}$  is also affected by power divergences, the subtraction  $O_{411} - O_{433}$  guarantees their removal. Another choice is  $\mu_1 \neq \mu_2 \neq \mu_3$ . In this case, the operator belongs to another irreducible representation of  $H(4)$  and renormalizes multiplicatively without introducing power divergences. However, this last example, while optimal in terms of renormalization, is far from optimal when calculating hadronic matrix elements<sup>2</sup>

$$\langle h(p) | O_{\{\mu_1 \dots \mu_n\}} | h(p) \rangle = p_{\mu_1} \dots p_{\mu_n} A_n^h(\mu) + \delta_{\mu_i \mu_j} \text{ terms}, \quad (10)$$

because it requires non-vanishing external momentum in at least 2 spatial directions. This substantially degrades the quality of the signal-to-noise ratio that is realized in numerical lattice QCD simulations. For  $O_{411} - O_{433}$ , one needs a non-vanishing external momentum in at least 1 spatial directions, and despite the subtraction of power divergences, one might hope to achieve a better signal-to-noise ratio. The operator with all the same indices has a power divergence that requires a complicated non-perturbative procedure to be subtracted and is not a viable solution. This is unfortunate because the matrix

element of  $O_{444}$ , for example, does not require any external spatial momentum and should be optimal in terms of the signal-to-noise ratio.

The mixing pattern becomes more cumbersome for higher dimensional operators,  $n \geq 4$ . For  $n = 4$ , choosing all 4 indices differently results in the only 2 irreducible representations: the totally symmetric and anti-symmetric representations. One then needs a non-vanishing external momentum in all 3 spatial directions to calculate the hadronic matrix elements[19]. For  $n > 4$ , mixings are unavoidable. The complicated renormalization pattern just described, together with the need of an external momentum to calculate the hadronic matrix elements, has, *de facto*, prevented the lattice calculation of the moments of parton distribution functions for  $n > 4$  and rendered the calculations for  $n = 3, 4$  challenging.

A very interesting idea to circumvent the renormalization issue, based on the recovery of the continuum rotational symmetry, was proposed in Ref. [21]. Even though the method was not further pursued numerically, it represents a first important step toward resolving the theoretical challenges encountered when calculating moments of PDFs.

**Gradient Flow** - The gradient flow (GF) for gauge and fermion fields [22–24] provides a different way to regulate short-distance singularities of the twist-2 operators. The connection with the physical renormalized matrix elements at vanishing flow time,  $t = 0$ , is obtained with a short-flow-time expansion (SFTX) after performing the continuum limit of the hadronic matrix elements at a fixed physical value of the flow time  $t$  [25].

The flowed twist-2 operators, written in terms of flowed fermions,  $\chi^r(x, t)$  and  $\bar{\chi}^r(x, t)$ , and gauge fields,  $B_\mu(x, t)$ , are given by

$$O_n^{rs}(x, t) = \bar{\chi}^r(x, t) \gamma_{\{\mu_1} \overleftrightarrow{D}_{\mu_2} \dots \overleftrightarrow{D}_{\mu_n\}} \chi^s(x, t), \quad (11)$$

where  $\{\dots\}$  denotes symmetrization (cf. Eq. (3)). These operators are particularly advantageous because they renormalize multiplicatively also on the lattice with a renormalization factor that depends only on the fermion content of the operator,

$$O_n^{rs}(t) = Z_n O_{n,B}^{rs}(t), \quad Z_n = Z_\chi, \quad (12)$$

where  $Z_\chi^{1/2}$  is the renormalization constant of the flowed fermion fields [24]. For correlation functions containing flowed twist-2 operators, the flow-time  $t$  provides a regulator for short-distance singularities. Beside the renormalization of the bare parameters of the theory, the flowed fermion fields, and any local field at  $t = 0$ , correlation functions do not require any additional renormalization. For lattice QCD applications, it is convenient to define  $Z_\chi$  in a scheme that is regularization independent, as then the matching and the renormalization can be performed in the same scheme. The choice of the specific scheme is not relevant for the general discussion, but it becomes important when calculating the matching coefficients. In the calculations of the matching coefficients described

<sup>1</sup> Strictly speaking,  $O_{411} - O_{433}$  belongs to an irreducible representation of  $H(4)$  that appears more than once. Therefore, a mixing between operators belonging to these equivalent representations can occur [19]. In perturbation theory the mixing seems to be numerically small.

<sup>2</sup> In Eq. (10) for simplicity we omit the flavor indices.

below, we renormalize the twist-2 operators using the so-called ringed fields [26], defined by the  $SU(N_c)$  gauge invariant and regularization independent condition

$$\left\langle \overset{\circ}{\chi}_r(x, t) \overset{\leftrightarrow}{D} \overset{\circ}{\chi}_r(x, t) \right\rangle = -\frac{N_c}{(4\pi)^2 t^2}. \quad (13)$$

Imposing this condition in dimensional regularization, with  $D = 4 - 2\epsilon$ , leads to a finite renormalization between the ringed fields and renormalized fields in the MS scheme

$$\begin{aligned} \chi_r(x, t) &= (8\pi t)^{\epsilon/2} \zeta_\chi^{1/2} \overset{\circ}{\chi}_r(x, t) \\ \bar{\chi}_r(x, t) &= (8\pi t)^{\epsilon/2} \zeta_\chi^{1/2} \overset{\circ}{\bar{\chi}}_r(x, t). \end{aligned} \quad (14)$$

The 1-loop result for the finite renormalization is given by [26]

$$\zeta_\chi = 1 - \frac{\bar{g}^2}{(4\pi)^2} C_F (3 \log(8\pi\mu^2 t) - \log(432)), \quad (15)$$

where  $\bar{g}$  is the strong coupling renormalized in the MS scheme at the renormalization scale  $\mu$ , and  $C_F = N_c^2 - 1/2N_c$ . This result has been extended to  $O(\bar{g}^4)$  in Refs. [27, 28]. Results obtained in the MS scheme can be converted to the  $\overline{\text{MS}}$  scheme by replacing the renormalization scale  $\mu$  with

$$\mu^2 = \bar{\mu}^2 \frac{e^{\gamma_E}}{(4\pi)}, \quad (16)$$

where  $\bar{\mu}$  is the renormalization scale in the  $\overline{\text{MS}}$  scheme.

*O(a) improvement* - The lattice QCD calculation of hadronic matrix elements of twist-2 operators is affected by cutoff effects. For non-perturbatively improved clover fermions, the hadronic matrix elements of the standard twist-2 operators (with  $t = 0$ ) are still affected by  $O(a)$  cutoff effects that could be removed by adopting an  $O(a)$  improved definition of the twist-2 operators. Excluding the case  $n = 2$ , where the corresponding improvement coefficients have been determined at 1-loop in perturbation theory [29], the continuum limit is reached with  $O(a)$  discretization effects.

If we consider flowed twist-2 operators for a generic  $n$ , the hadronic matrix elements are affected only by  $O(am)$  cutoff effects, where  $m$  is the quark mass. Additional improvement coefficients specific to the twist-2 operators are not needed. In the discussion of the method's applications below, we also consider ratios of flowed matrix elements where both  $Z_\chi$  and the  $O(am)$  cutoff effects are eliminated. In summary, regardless of the lattice setup adopted, the use of flowed twist-2 operators provides a significant simplification in the renormalization pattern. Moreover, for non-perturbatively improved clover fermions, it also improves the parametric scaling towards the continuum limit.

**Matching coefficients** - After performing the continuum limit of the hadronic matrix element for a fixed  $t > 0$  value of the flow time, the connection with physical renormalized matrix element at  $t = 0$  is obtained

with a SFTX [25]. The SFTX of the twist-2 operators  $O_n(x, t)$ , in general contains power divergences with terms like  $1/t^m \delta_{\mu_i \mu_j}$ , where  $m = (d_n - d_p)/2$  depends on the dimensions of  $O_n$ ,  $d_n$ , and on the dimension of the lower-dimensional operator,  $d_p$ . These terms, though, are classified using the continuum  $O(4)$  symmetry and, as a result, the SFTX of the symmetrized and traceless operators,  $\widehat{O}_n$ , receives contributions only from the corresponding traceless operators at  $t = 0$ .

We renormalize the flowed fermion fields adopting ringed fields, introduced in the previous section, and define the ringed twist-2 operators

$$\begin{aligned} \widehat{O}_n^{rs}(x, t) &= \overset{\circ}{\chi}^r(x, t) \gamma_{\{\mu_1} \overset{\leftrightarrow}{D}_{\mu_2} \cdots \overset{\leftrightarrow}{D}_{\mu_n\}} \overset{\circ}{\chi}^s(x, t) - \\ &\quad - \text{terms with } \delta_{\mu_i \mu_j}, \end{aligned} \quad (17)$$

where the subtraction guarantees that the resulting operator has vanishing traces. The SFTX of  $\widehat{O}_n^{rs}$  is

$$\widehat{O}_n^{rs}(t) = c_n(t, \mu) \widehat{O}_{n, \text{MS}}^{rs}(\mu) + \cdots, \quad (18)$$

where we make explicit only the dependence on the flow time and the renormalization scale. The neglected terms are higher-order contributions of positive powers of  $t$ .

The matching coefficients are determined considering off-shell amputated one-particle irreducible (1PI) Green's functions containing the flowed operators  $\widehat{O}_n^{rs}(t)$ . The matching equations with massless fermions

$$\left\langle \psi^r \widehat{O}_n^{rs}(t) \bar{\psi}^s \right\rangle = c_n(t, \mu) \left\langle \psi^r \widehat{O}_{n, \text{MS}}^{rs}(t=0, \mu) \bar{\psi}^s \right\rangle \quad (19)$$

are solved in  $D = 4 - 2\epsilon$  at 1-loop in perturbation theory with

$$c_n(t, \mu) = 1 + \frac{\bar{g}^2(\mu)}{(4\pi)^2} c_n^{(1)}(t, \mu) + O(\bar{g}^4). \quad (20)$$

The matching coefficients  $c_n(t, \mu)$  depend on the renormalized coupling and are independent of the soft scales. For their calculation, one uses standard techniques (see for example Ref. [30] and Refs. therein), expanding the integrands of the loop integrals of the matching equations (19) in all soft scales keeping  $t$  fixed. The  $t = 0$  1-loop contribution on the r.h.s of Eq. (19) vanishes because the expansion leads to scaleless, i.e. vanishing, integrals in D-dimensions. After renormalizing the gauge coupling and the flowed fermion fields, the left-hand side is UV finite. The infrared singularities stemming from the expansion in the soft scales, and regulated in dimensional regularization, match exactly the UV poles of  $Z_n^{\text{MS}}$ . The finite matching coefficients are the result of this procedure.

The Feynman diagrams contributing are depicted <sup>3</sup> in Fig. 1. The cross indicates the insertion of the twist-2

<sup>3</sup> To draw the Feynman diagrams we have used FeynGame [31].

operators, the single straight and wavy lines respectively represent the fermion and gluon propagator, and the double straight lines represent the kernel of the fermionic GF operator. The open circle represents a GF vertex, and the rest are standard QCD vertices. The Feynman rules for the operators are the same as in the unflowed case, and the remaining Feynman rules related to the expansion of the GF equation can be found, for example, in Refs. [30, 32]. The final result for the matching coefficients is

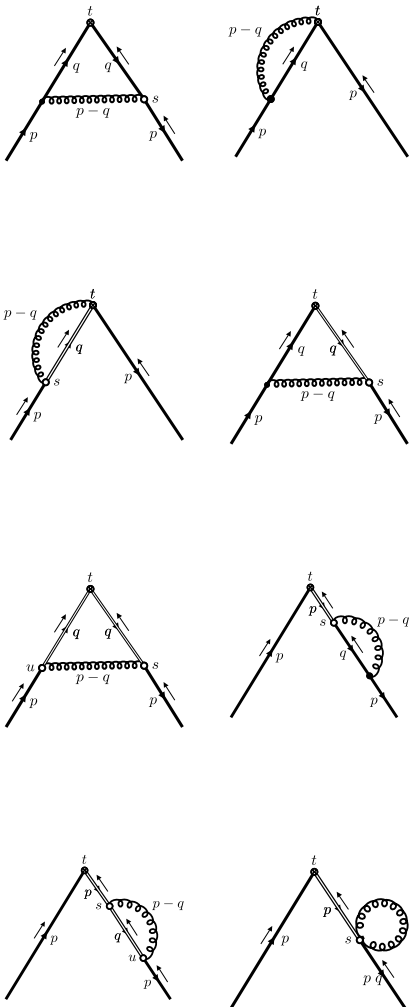


FIG. 1. Feynman diagram for the  $O(\bar{g}^2)$  calculations of the matching coefficients in Eq. (19). The circle with the cross represents the twist-2 operator and the empty circles the GF vertices. The double line represents the fermionic kernel of the GF differential operator. The arrows beside the fermion lines and the kernel lines indicate the direction of increasing flow time.

$$c_n^{(1)}(t, \mu) = C_F [\gamma_n \log(8\pi\mu^2 t) + B_n], \quad (21)$$

where

$$\gamma_n = 1 + 4 \sum_{j=2}^n \frac{1}{j} - \frac{2}{n(n+1)}, \quad (22)$$

and

$$\begin{aligned} B_n = & \frac{4}{n(n+1)} + 4 \frac{n-1}{n} \log 2 + \frac{2-4n^2}{n(n+1)} \gamma_E - \\ & - \frac{2}{n(n+1)} \psi(n+2) + \frac{4}{n} \psi(n+1) - 4\psi(2) - \\ & - 4 \sum_{j=2}^n \frac{1}{j(j-1)} \frac{1}{2^j} \phi(1/2, 1, j) - \log(432). \quad (23) \end{aligned}$$

In this expression  $\gamma_E = 0.57221\dots$  is the Euler's constant,  $\psi(z)$  is the digamma function, and  $\phi(z, s, a)$  is the Lerch transcendent defined as  $\phi(z, s, a) = \sum_{k=0}^{\infty} \frac{z^k}{(k+a)^s}$ .

The expression for  $\gamma_n$  matches the 1-loop anomalous dimension of the twist-2 operators [33] and provides a welcome check of the calculation. For  $n > 2$  the finite part,  $B_n$ , in Eq. (23) provides a new result. The result with  $n = 2$  was already obtained in Ref. [26] in the analysis of the energy-momentum tensor, and we reproduce their result.

The fact that the matching of the flowed matrix elements is so simple opens the possibility of computing moments of the parton distribution functions of any order. A possible operational procedure is the following: After fixing  $n$ , one constructs the symmetric and traceless operator  $\hat{O}_n^{rs}$ . One proceeds calculating the matrix elements between hadron states of

$$\left\langle h(p) | \hat{O}_n^{rs}(t) | h(p) \right\rangle, \quad (24)$$

using standard techniques based on the spectral decomposition. To apply the decomposition in the lattice calculation of the 3-point function, one needs to ensure that the physical distance between the interpolators of the hadron states and of the flowed operators is much larger than the flow-time radius  $\sqrt{8t}$ . After performing the continuum limit, the renormalized matrix element in the MS scheme is calculated simply by

$$A_n^{\text{MS}}(\mu) = c_n(t, \mu)^{-1} A_n(t). \quad (25)$$

This matching is correct only if the flowed fields are defined as ringed fields. If the flowed fields are renormalized in a different scheme, the finite part of the matching coefficient has to be modified.

If the matching is successful, the l.h.s of Eq. (25) should be independent of the flow time. Violations stem from higher dimensional operators as linear terms in  $t$ , and from higher order terms in the perturbative expansion of the matching coefficients. To mitigate these possible systematics it is important to extend to  $O(\bar{g}^4)$  the calculation presented here and conduct a thorough numerical

study of the residual flow-time dependence of the hadronic matrix element after the matching.

**Applications** - The simplicity of the matching is guaranteed once the operators are symmetrized on the Lorentz indices, and all the traces have been subtracted. In the case of  $n = 3$ , the traceless operator is

$$\widehat{O}_3^{rs} = \widehat{O}_{\{\mu_1\mu_2\mu_3\}}^{rs} = O_{\{\mu_1\mu_2\mu_3\}}^{rs} - \frac{1}{6} \left[ \delta_{\mu_1\mu_2} O_{\{\alpha\alpha\mu_3\}}^{rs} + \delta_{\mu_1\mu_3} O_{\{\alpha\mu_2\alpha\}}^{rs} + \delta_{\mu_2\mu_3} O_{\{\mu_1\alpha\alpha\}}^{rs} \right] \quad (26)$$

where repeated indices are summed over. This implies that for example we can now choose  $\mu_1 = \mu_2 = \mu_3 = 4$  and calculate the matrix element of

$$\widehat{O}_{444} = \frac{1}{2} \left[ O_{444} - \frac{1}{3} (O_{kk4} + O_{k4k} + O_{4kk}) \right]. \quad (27)$$

The hadronic matrix element of  $\widehat{O}_{444}(t)$  is calculable with vanishing external momentum and, at finite flow time, it renormalizes multiplicatively. The matching with the MS scheme at renormalization scale  $\mu$  is obtained using Eq. (25). In a similar way, traceless operators for any  $n$  can be constructed. To exemplify how to construct traceless operators, for  $n = 4$  we have

$$\widehat{O}_{4444} = O_{4444} - \frac{3}{4} O_{\{\alpha\alpha 44\}} + \frac{1}{16} O_{\{\alpha\alpha\beta\beta\}}. \quad (28)$$

Again the hadronic matrix element of  $\widehat{O}_{4444}(t)$  is calculable with no external spatial momentum, and the matching with the MS operator is multiplicative.

The continuum limit of the reduced hadronic matrix element of  $\widehat{O}_n$ , denoted as  $A_n^h(t) = \langle x^{n-1} \rangle^h(t)$ , would require a determination of  $Z_\chi$  from lattice QCD simulations. However, this can be avoided taking the second moment  $A_2^{h,MS}(\mu) = \langle x \rangle_{MS}^h(\mu)$  as already computed with any method of choice. Then all the other moments for  $n > 2$  are calculable from

$$\langle x^{n-1} \rangle_{MS}^h(\mu) = \langle x \rangle_{MS}^h(\mu) \frac{c_2(t, \mu)}{c_n(t, \mu)} \frac{\langle x^{n-1} \rangle^h(t)}{\langle x \rangle^h(t)}, \quad (29)$$

where  $c_2(t, \mu)$  and  $c_n(t, \mu)$  are given by Eqs. (21-23).

The ratios  $\frac{\langle x^{n-1} \rangle^h(t)}{\langle x \rangle^h(t)}$  have a finite continuum limit, and there is no need to renormalize the flowed fields. Moreover, these ratios exhibit  $O(a^2)$  scaling violations once the lattice theory has been non-pertubatively improved. If convenient numerically, it is also possible to use different hadrons for the  $n$ -th and the second moment matrix elements in Eq. (29) because the matching coefficients

are independent on the hadron for which we calculate the matrix element.

The gradient flow has been previously employed to define quasi-PDF in [34], and the 1-loop matching has been calculated in [35]. While, in principle, the determination of moments of PDFs should allow a precise reconstruction of the PDFs, it would be intriguing to explore whether the determination of the PDF moments outlined in this work can be integrated with quasi-PDF calculations.

**Summary** - We have described a method that resolves both the theoretical and numerical challenges faced when calculating moments of parton distribution functions from lattice QCD. A lattice regulator breaks the Euclidean rotational symmetry into the hypercubic group. As a result, the renormalization of twist-2 operators on the lattice is a substantial hurdle to determine moments of parton distribution functions  $\langle x^{n-1} \rangle$ . For  $n > 4$ , power divergences in the lattice spacing are unavoidable, and for  $n = 3, 4$  the cancellation of power divergences is still possible by choosing suitable irreducible representations of the hypercubic group. The price to pay is that the calculation of the hadronic matrix elements necessitates the use of a spatial external momentum, worsening the signal-to-noise ratio of the correlation functions. At finite flow time  $t$ , the correlation functions of twist-2 operators are finite once the bare parameters of the theory and the flowed fermion fields are renormalized. After performing the continuum limit, the matching with the physical matrix element can be done at short flow time using the continuum symmetries of the theory. Using traceless and symmetrized operators guarantees that the matching is multiplicative, and we have calculated, at 1-loop in perturbation theory, the matching coefficients. This result opens the way to determine moments of any order of the parton distribution functions. While, in principle, this enables the reconstruction of PDFs from lattice QCD simulations, it would be very interesting to investigate how the approach described in this work can complement recent efforts aimed at the direct determination of PDFs from lattice QCD correlators.

*Acknowledgments* I would like to thank Andre Walker-Loud for constant encouragement and a critical reading of the manuscript. I also thank R. Harlander and T. Luu for suggestions on how to improve the original draft. I have benefited from many discussions about the gradient flow with R. Harlander, J. Kim, T. Luu, E. Mereghetti, C. Monahan, M. Rizik, P. Stoffer and A. Walker-Loud. I want to thank the Nuclear Theory Group of the Lawrence Berkeley National Lab and the University of California Berkeley for their hospitality. I acknowledge funding support from Deutsche Forschungsgemeinschaft (DFG, German Research Foundation) through grant 513989149 and under the National Science Foundation grant PHY-2209185.

[1] J. C. Collins, D. E. Soper, and G. F. Sterman, Factorization of Hard Processes in QCD, Adv. Ser.

- arXiv:hep-ph/0409313.
- [2] V. N. Gribov and L. N. Lipatov, Deep inelastic e p scattering in perturbation theory, *Sov. J. Nucl. Phys.* **15**, 438 (1972).
- [3] L. N. Lipatov, The parton model and perturbation theory, *Yad. Fiz.* **20**, 181 (1974).
- [4] Y. L. Dokshitzer, Calculation of the Structure Functions for Deep Inelastic Scattering and e+ e- Annihilation by Perturbation Theory in Quantum Chromodynamics., *Sov. Phys. JETP* **46**, 641 (1977).
- [5] G. Altarelli and G. Parisi, Asymptotic Freedom in Parton Language, *Nucl. Phys. B* **126**, 298 (1977).
- [6] G. Curci, W. Furmanski, and R. Petronzio, Evolution of Parton Densities Beyond Leading Order: The Nonsinglet Case, *Nucl. Phys. B* **175**, 27 (1980).
- [7] J. C. Collins and D. E. Soper, Parton Distribution and Decay Functions, *Nucl. Phys. B* **194**, 445 (1982).
- [8] A. S. Kronfeld and D. M. Photiadis, Phenomenology on the Lattice: Composite Operators in Lattice Gauge Theory, *Phys. Rev. D* **31**, 2939 (1985).
- [9] G. Martinelli and C. T. Sachrajda, Pion Structure Functions From Lattice QCD, *Phys. Lett. B* **196**, 184 (1987).
- [10] G. Martinelli and C. T. Sachrajda, A Lattice Calculation of the Pion's Form-Factor and Structure Function, *Nucl. Phys. B* **306**, 865 (1988).
- [11] U. Aglietti, M. Ciuchini, G. Corbo, E. Franco, G. Martinelli, and L. Silvestrini, Model independent determination of the shape function for inclusive B decays and of the structure functions in DIS, *Phys. Lett. B* **432**, 411 (1998), arXiv:hep-ph/9804416.
- [12] W. Detmold and C. J. D. Lin, Deep-inelastic scattering and the operator product expansion in lattice QCD, *Phys. Rev. D* **73**, 014501 (2006), arXiv:hep-lat/0507007.
- [13] X. Ji, Parton Physics on a Euclidean Lattice, *Phys. Rev. Lett.* **110**, 262002 (2013), arXiv:1305.1539 [hep-ph].
- [14] A. Radyushkin, Nonperturbative Evolution of Parton Quasi-Distributions, *Phys. Lett. B* **767**, 314 (2017), arXiv:1612.05170 [hep-ph].
- [15] A. J. Chambers, R. Horsley, Y. Nakamura, H. Perlt, P. E. L. Rakow, G. Schierholz, A. Schiller, K. Somfleth, R. D. Young, and J. M. Zanotti, Nucleon Structure Functions from Operator Product Expansion on the Lattice, *Phys. Rev. Lett.* **118**, 242001 (2017), arXiv:1703.01153 [hep-lat].
- [16] Y.-Q. Ma and J.-W. Qiu, Extracting Parton Distribution Functions from Lattice QCD Calculations, *Phys. Rev. D* **98**, 074021 (2018), arXiv:1404.6860 [hep-ph].
- [17] J. Liang, T. Draper, K.-F. Liu, A. Rothkopf, and Y.-B. Yang (XQCD), Towards the nucleon hadronic tensor from lattice QCD, *Phys. Rev. D* **101**, 114503 (2020), arXiv:1906.05312 [hep-ph].
- [18] M. Hamermesh, Group Theory and Its Application to Physical Problems, Addison-Wesley series in physics (Addison-Wesley Publishing Company, 1962).
- [19] G. Beccarini, M. Bianchi, S. Capitani, and G. Rossi, Deep inelastic scattering in improved lattice QCD. 2. The second moment of structure functions, *Nucl. Phys. B* **456**, 271 (1995), arXiv:hep-lat/9506021.
- [20] M. Gockeler, R. Horsley, E.-M. Ilgenfritz, H. Perlt, P. E. L. Rakow, G. Schierholz, and A. Schiller, Lattice operators for moments of the structure functions and their transformation under the hypercubic group, *Phys. Rev. D* **54**, 5705 (1996), arXiv:hep-lat/9602029.
- [21] Z. Davoudi and M. J. Savage, Restoration of Rotational Symmetry in the Continuum Limit of Lattice Field Theories, *Phys. Rev. D* **86**, 054505 (2012), arXiv:1204.4146 [hep-lat].
- [22] Lüscher, M., Properties and uses of the Wilson flow in lattice QCD, *JHEP* **1008**, 071, arXiv:1006.4518 [hep-lat].
- [23] Lüscher, M. and P. Weisz, Perturbative analysis of the gradient flow in non-abelian gauge theories, *JHEP* **1102**, 051, arXiv:1101.0963 [hep-th].
- [24] Lüscher, M., Chiral symmetry and the Yang–Mills gradient flow, *JHEP* **1304**, 123, arXiv:1302.5246 [hep-lat].
- [25] M. Lüscher, Future applications of the Yang-Mills gradient flow in lattice QCD, *PoS LATTICE2013*, 016 (2014), arXiv:1308.5598 [hep-lat].
- [26] H. Makino and H. Suzuki, Lattice energy–momentum tensor from the Yang-Mills gradient flow–inclusion of fermion fields, *PTEP* **2014**, 063B02 (2014), arXiv:1403.4772 [hep-lat].
- [27] R. V. Harlander, Y. Kluth, and F. Lange, The two-loop energy–momentum tensor within the gradient-flow formalism, *Eur. Phys. J. C* **78**, 944 (2018), [Erratum: *Eur. Phys. J. C* **79**, no.10, 858 (2019)], arXiv:1808.09837 [hep-lat].
- [28] J. Artz, R. V. Harlander, F. Lange, T. Neumann, and M. Prausa, Results and techniques for higher order calculations within the gradient-flow formalism, *JHEP* **06**, 121, [erratum: *JHEP* **10**, 032 (2019)], arXiv:1905.00882 [hep-lat].
- [29] S. Capitani, M. Gockeler, R. Horsley, H. Perlt, P. E. L. Rakow, G. Schierholz, and A. Schiller, Renormalization and off-shell improvement in lattice perturbation theory, *Nucl. Phys. B* **593**, 183 (2001), arXiv:hep-lat/0007004.
- [30] E. Mereghetti, C. J. Monahan, M. D. Rizik, A. Shindler, and P. Stoffer, One-loop matching for quark dipole operators in a gradient-flow scheme, *JHEP* **04**, 050, arXiv:2111.11449 [hep-lat].
- [31] R. V. Harlander, S. Y. Klein, and M. Lipp, *FeynGame*, *Comput. Phys. Commun.* **256**, 107465 (2020), arXiv:2003.00896 [physics.ed-ph].
- [32] M. D. Rizik, C. J. Monahan, and A. Shindler (SymLat), Short flow-time coefficients of CP-violating operators, *Phys. Rev. D* **102**, 034509 (2020), arXiv:2005.04199 [hep-lat].
- [33] D. J. Gross and F. Wilczek, ASYMPTOTICALLY FREE GAUGE THEORIES. 2., *Phys. Rev. D* **9**, 980 (1974).
- [34] C. Monahan and K. Orginos, Quasi parton distributions and the gradient flow, *JHEP* **03**, 116, arXiv:1612.01584 [hep-lat].
- [35] C. Monahan, Smeared quasidistributions in perturbation theory, *Phys. Rev. D* **97**, 054507 (2018), arXiv:1710.04607 [hep-lat].